

# Measuring rare and exclusive Higgs boson decays into light resonances

Andrew S. Chisholm<sup>a,1</sup>, Silvan Kuttimalai<sup>b,2</sup>, Konstantinos Nikolopoulos<sup>c,1</sup>,  
Michael Spannowsky<sup>d,2</sup>

<sup>1</sup>School of Physics and Astronomy,  
University of Birmingham, B15 2TT, United Kingdom

<sup>2</sup>Institute for Particle Physics Phenomenology, Department of Physics,  
Durham University, DH1 3LE, United Kingdom

the date of receipt and acceptance should be inserted later

**Abstract** We evaluate the LHC's potential of observing Higgs boson decays into light elementary or composite resonances through their hadronic decay channels. We focus on the Higgs boson production processes with the largest cross sections,  $pp \rightarrow h$  and  $pp \rightarrow h + \text{jet}$ , with subsequent decays  $h \rightarrow ZA$  or  $h \rightarrow Z\eta_c$ , and comment on the production process  $pp \rightarrow hZ$ . By exploiting track-based jet substructure observables and extrapolating to  $3000 \text{ fb}^{-1}$  we find  $\mathcal{BR}(h \rightarrow ZA) \simeq \mathcal{BR}(h \rightarrow Z\eta_c) \lesssim 0.02$  at 95 % CL. We interpret this limit in terms of the 2HDM Type 1. We find that searches for  $h \rightarrow ZA$  are complementary to existing measurements and can constrain large parts of the currently allowed parameter space.

## 1 Introduction

The greatly successful Run 1 of the large hadron collider (LHC) culminated in the discovery of a state that resembles the standard model (SM) Higgs boson [1, 2]. First measurements of its couplings to gauge bosons and third-generation fermions are in good agreement with SM predictions [3]. However, the current precision of the measurement of Higgs boson couplings and properties cannot rule out Higgs boson decays into light resonances. In the SM, examples of such light resonances include the composite unflavoured mesons and quarkonium states, e.g. the  $J/\psi$ .

Furthermore, Higgs boson decays into elementary light resonances are predicted by many extensions of

the SM [4]. They arise generically in scenarios with multiple Higgs fields or kinetic mixing between SM gauge bosons and bosons of a dark  $U(1)$  gauge group. In the NMSSM, Higgs boson decays into an additional light CP-odd scalar can occur. Close to the alignment limit of the Two-Higgs-Doublet Model (2HDM) of Type I or II, a light CP-odd scalar with mass of few GeV can also be phenomenologically accommodated with a 125 GeV SM-like Higgs boson  $h$  [5]. Higgs boson decays into vector bosons of the SM and an additional spontaneously broken  $U(1)_D$  [6] can arise through kinetic mixing induced by heavy particles that carry hypercharge, e.g.  $h \rightarrow ZZ_D$  or  $h \rightarrow \gamma Z_D$ .

Searches for light composite resonances have been proposed to set a limit on the Higgs boson couplings to first and second-generation quarks [7, 8]. However, for SM couplings the branching ratios for exclusive Higgs boson decays are generally of  $\mathcal{O}(10^{-5})$  or less [7, 9, 10], e.g.  $\mathcal{BR}(h \rightarrow Z\eta_c) \simeq 1.4 \times 10^{-5}$ ,  $\mathcal{BR}(h \rightarrow \rho^0\gamma) \simeq 1.68 \times 10^{-5}$  or  $\mathcal{BR}(h \rightarrow J/\psi \gamma) \simeq 2.95 \times 10^{-6}$ , resulting in small expected event yields. Nevertheless, both general purpose experiments at the LHC have performed searches for exclusive Higgs boson decays, focusing on the dimuon decays of vector quarkonia. With Run 1 data the ATLAS collaboration has set 95 % confidence level (CL) upper limits of  $\mathcal{O}(10^{-3})$  on the branching ratios for  $\mathcal{BR}(h \rightarrow J/\psi \gamma)$  and  $\mathcal{BR}(h \rightarrow \Upsilon(1S, 2S, 3S) \gamma)$  [11], while the CMS collaboration obtained a similar upper limit for  $\mathcal{BR}(h \rightarrow J/\psi \gamma)$  [12]. Recently, the ATLAS collaboration has also set a 95 % CL upper limit of  $1.4 \times 10^{-3}$  on  $\mathcal{BR}(h \rightarrow \phi \gamma)$  [13].

Hence, rare decays of Higgs bosons into light elementary or composite resonances are of direct relevance for the two most important tasks of the upcoming LHC runs: (a) precision measurements of the Higgs boson properties; and (b) searches for new physics.

<sup>a</sup>Andrew.Chisholm@cern.ch

<sup>b</sup>s.s.kuttimalai@durham.ac.uk

<sup>c</sup>k.nikolopoulos@bham.ac.uk

<sup>d</sup>michael.spannowsky@durham.ac.uk

While most existing search strategies rely upon resonance decays into leptons, i.e. muons, the total width of most composite resonances and elementary scalars is dominated by decays into hadronic final states, e.g.  $\mathcal{BR}(\eta_c \rightarrow \text{hadrons}) > 52\%*$  [14]. Instead of exploiting only leptonic decay modes, we therefore propose that the inclusive hadronic decays be considered. Light resonances  $X$  with masses of  $m_X = 1 - 10$  GeV produced in decays of the Higgs boson with a mass of 125 GeV, are highly boosted and their decay products are thus confined within a small area of the detector. The angular separation of the decay products of the resonance  $X$  scales like  $\Delta R = \sqrt{\Delta\eta^2 + \Delta\phi^2} \sim 4m_X/m_h$ , where  $\eta$  is the pseudorapidity and  $\phi$  the azimuthal angle. Separating the decay products in the calorimeters of the detector poses a challenge, as the typical size of hadronic calorimeter cells is  $0.1 \times 0.1$  in the  $(\eta, \phi)$  plane.

Thus, to discriminate two jets the angular separation of their axes has to be roughly  $\Delta R \gtrsim 0.2$ . If opening angles are smaller, the total energy deposit of the resonance decay products can still be measured, but the substructure, i.e. the energy sharing between the decay products, becomes opaque. To maintain the ability to separate between signal and QCD-induced backgrounds we propose to utilise track-based reconstruction. Trajectories of charged particles as measured in the tracking detectors provide a much better spatial resolution than the reconstructed calorimeter clusters. Recently, a similar approach was advocated for highly boosted electroweak scale resonances [15–18], for which dedicated taggers have been developed.<sup>†</sup>

In this work, we use track-based reconstruction techniques to evaluate the sensitivity of general purpose detectors at hadron colliders, with characteristics similar to those of ATLAS [19] and CMS [20], in measuring rare Higgs boson decays into light hadronically decaying resonances. Focusing on the High Luminosity LHC (HL-LHC) regime, our analysis assumes a dataset corresponding to an integrated luminosity of  $3000 \text{ fb}^{-1}$  collected at center-of-mass energy  $\sqrt{s} = 13 \text{ TeV}$ . We consider two production channels for the Higgs boson: inclusive Higgs boson production and Higgs boson production in association with a hard jet of transverse momentum  $p_T > 150 \text{ GeV}$ .

As two benchmark cases for rare Higgs boson decays into light resonances we consider  $h \rightarrow Z(\rightarrow \ell\ell) + \eta_c$  and  $h \rightarrow Z(\rightarrow \ell\ell) + A$ , where  $A$  is assumed to be an elementary CP-odd scalar of mass 4 GeV which decays mostly hadronically. The presence of two high-pT isolated lep-

tons from the Z boson decay, ensure an efficient trigger strategy for HL-LHC environment. The characteristics of the  $h \rightarrow Z(\rightarrow \ell\ell) + \eta_c$  benchmark are expected to be representative of similar decays to vector charmonia (e.g.  $h \rightarrow Z(\rightarrow \ell\ell) + J/\psi$ ), due to similarities in their hadronic decay patterns and small mass differences relative to the scale of the jet momenta relevant in the decays of Higgs boson with a mass of 125 GeV.

The event generation is described in Sect. 2, while Sect. 3 is devoted to the details of the reconstruction of the Higgs boson decay products and event selection. The statistical analysis and expected sensitivity are given in Sect. 4. In Sect. 5 the expected results are interpreted in terms of 2HDM models. We offer a summary of our findings in Sect. 6.

## 2 Event generation

For the simulation of both the signal and the background contributions we employ a modified version of Sherpa 2.2.0 [21] that was adapted in such a way as to facilitate the simulation of Higgs decays into composite resonances. Parton shower effects, hadronisation, as well as underlying event contributions are taken into account throughout. Both Higgs boson production processes,  $h + \text{jet}$  and inclusive  $h$ , are calculated at NLO and matched to the parton shower. Finite top quark mass effects in the gluon fusion production mechanism are taken into account as described in Ref. [22]. The Higgs boson decays  $h \rightarrow Z\eta_c$ ,  $h \rightarrow ZA$  as well as the subsequent decay of the pseudoscalar and the Z boson are calculated perturbatively at leading order using the algorithm and methods described in Ref. [23]. Spin-correlations are thus retained in all resonance decays. The UFO model format, supported by Sherpa, was used for the implementation of an elementary pseudoscalar and its interactions [23, 24].

The  $Z + \text{jets}$  production is expected to represent the dominant background in this search with other contributions such as  $t\bar{t}$  production being suppressed to a negligible level by requiring an opposite-charge same-flavour dilepton with an invariant mass consistent with the Z boson mass. For inclusive Z boson production ( $Z + \text{jets}$ ), we take into account the full dilepton final state in the matrix elements and calculate the core process at NLO. We account for additional hard jet emissions by means of multijet merging techniques [25] and include leading order matrix elements with up to two additional jets in the setup.

We process the generated events with the DELPHES fast simulation framework [26], which uses parametrised descriptions of the response of particle physics detectors

\*Based on a simple sum of the branching fractions for the observed decays of the  $\eta_c$  into stable hadrons.

<sup>†</sup><http://www.ippp.dur.ac.uk/~mspannow/webipp/HPTTaggers.html>

to provide reconstructed physics objects, allowing a realistic data analyses to be performed. As an example of a general purpose LHC detector, the default ATLAS configuration card included in DELPHES is used.

### 3 Reconstruction setup and selection

#### 3.1 Leptonic $Z$ boson decay reconstruction

The reconstruction of  $Z \rightarrow \ell\ell$  decays begins with the identification of isolated lepton (electron or muon) candidates. Reconstructed leptons are required to satisfy  $p_T > 8 \text{ GeV}$  and  $|\eta| < 2.5$ , one lepton is required to fulfill a trigger requirement of  $p_T > 25 \text{ GeV}$ . An isolation requirement based on the presence of reconstructed tracks and calorimeter deposits within  $\Delta R < 0.2$  of a lepton is imposed. The sum of the transverse momentum of such objects is required to be less than 10 % of the  $p_T$  of the lepton itself. Oppositely charged pairs of isolated leptons, which satisfy  $81 \text{ GeV} < m_{\ell\ell} < 101 \text{ GeV}$  are identified as  $Z$  boson candidates.

#### 3.2 Hadronic resonance reconstruction

The reconstruction of hadronically decaying resonances within events begins with a search for anti- $k_t$  calorimeter jets with  $R = 0.4$ , seeded by clusters of calorimeter energy deposits. Calorimeter jets are required to have  $p_T > 30 \text{ GeV}$  and  $|\eta| < 2.5$ . Any jets which are within  $\Delta R < 0.3$  of leptons forming a  $Z \rightarrow \ell\ell$  candidate are rejected. Following the identification of such a jet, the jet constituents are used to seed a search for an anti- $k_t$  calorimeter jet with  $R = 0.2$ . The identification of an  $R = 0.2$  jet from the constituents of the initial  $R = 0.4$  jet is required to be successful. This procedure, i.e. the reconstruction of anti- $k_t$   $R = 0.2$  jets from the constituents of identified  $R = 0.4$  jets, is repeated for track jets, seeded by reconstructed charged particles. Track jets are associated to calorimeter jets by a simple spatial matching, based on a requirement of  $\Delta R < 0.4$  between the axes of the  $R = 0.4$  calorimeter and track jets. Only jets reconstructed with both calorimeter and track components are considered for further analysis and at least one such jet is required to be reconstructed.

To distinguish hadronically decaying charmonium states or light scalars from the copious production of low  $p_T$  jets, a boosted decision tree (BDT) is used through the TMVA package [27]. The following variables are used as input to the BDT:

- The  $p_T$  of the  $R = 0.4$  track and calorimeter jets, as the Higgs boson decay products are expected to have a harder jet  $p_T$  spectrum.
- The masses of the  $R = 0.4$  and  $R = 0.2$  track and calorimeter jets, as the jets in the signal are expected to be close to the mass of the light resonance.
- The number of track constituents associated with the  $R = 0.4$  and  $R = 0.2$  track jets, as the signal is expected to have a lower track multiplicity given the upper bound imposed by the light resonance mass.
- The ratio of the  $R = 0.2$  calorimeter (track) jets  $p_T$  to the  $p_T$  of the associated  $R = 0.4$  calorimeter (track) jet, this quantity is expected to prefer values more toward unity in the signal case where a narrow boosted topology is expected, a wider distribution expected from the QCD jet background.
- The spatial separation,  $\Delta R$ , between the leading  $p_T$  track within the  $R = 0.4$  track jet and the jet axis.
- The ratio of the highest track  $p_T$  to the  $p_T$  of the  $R = 0.4$  track jet.

The final variables are designed to exploit the fact that in the signal we find on average fewer charged tracks and, due to the very small resonance mass, a smaller active area of the jet.

The performance of the BDT is summarised in Fig. 1, where the background rejection is shown as a function of the signal efficiency. Higgs decays into a composite light resonance  $\eta_c$  and Higgs decays into an elementary pseudoscalar  $A$ , which in turn decays hadronically, are considered separately. For the elementary pseudoscalar, individual curves for the case in which it decays into a pair of quarks ( $c\bar{c}$  taken as an example) and for the case in which it decays into a pair of gluons are shown. These pseudoscalar decay modes will be of relevance for the interpretation of our results in the context of 2HDMs in Sect. 5. Examples of the distributions of the variables used to train the BDT are shown in Fig. 2. The most important variables in terms of discrimination between signal and background are found to be the jet masses, followed by the number of track constituents associated with the track jets.

#### 3.3 Selection of $h \rightarrow ZA$ and $h \rightarrow Z\eta_c$ decays

Events containing at least one hadronic decay candidate and one  $Z \rightarrow \ell\ell$  candidate are considered for further analysis. In the case of the  $h + \text{jet}$  production channel, an additional  $R = 0.4$  anti- $k_t$  calorimeter jet with  $p_T > 150 \text{ GeV}$  and  $|\eta| < 2.5$  is required (no substructure or matching track jet is required). The single  $Z$  boson candidate with  $m_{\ell\ell}$  closest to the  $Z$  boson mass is chosen to form the  $h \rightarrow ZA(\eta_c)$  candidate. If multiple hadronic decay candidates are reconstructed, the candidate which when paired with the  $Z \rightarrow \ell\ell$  candidate has an invariant mass closest to  $m_h = 125 \text{ GeV}$  is

chosen. Finally, the transverse momentum of the  $h$  candidate is required to exceed 20 GeV. The invariant mass of the jet–dilepton system is shown for the inclusive and  $h$  + jet production channels in Fig. 3.

The BDT response is shown for both the signal and the background contributions to the inclusive and  $h$  + jet production channels in Fig. 4.

#### 4 Statistical analysis and results

The expected performance of the analysis is used to evaluate expected 95 % CL limits on the branching fractions  $\mathcal{BR}(h \rightarrow ZA)$ , in the cases where  $\mathcal{BR}(A \rightarrow gg) = 1.0$  or  $\mathcal{BR}(A \rightarrow c\bar{c}) = 1.0$ , and  $\mathcal{BR}(h \rightarrow Z\eta_c)$ . The yields of signal and background events within  $110 \text{ GeV} < m_{\ell\ell j} < 140 \text{ GeV}$  are used to evaluate the limits. To exploit the additional sensitivity offered by the BDT, a requirement on the BDT response is imposed. The value of this requirement is optimised to provide the best limit on the branching fractions of interest. The expected 95 % CL limits on the branching fractions of interest are shown Table 1. Branching fraction limits at the 1 % level can be expected. The inclusive production channel is found to be slightly more sensitive than the  $h$  + jet channel.

In addition to the channels described, Higgs boson production in association with a leptonically decaying  $Z$  boson was also considered as a possible channel to gain additional sensitivity. Initial studies into this channel demonstrated improved signal-to-background ratios when compared to the two channels constituting the main study, though the substantially lower number of signal events resulted in expected branching fraction limits that were up to an order of magnitude higher than the inclusive and  $h$  + jet channels.

Channel	$\mathcal{BR}$ 95 % confidence level upper limit		
	$h \rightarrow ZA(\rightarrow gg)$	$h \rightarrow ZA(\rightarrow c\bar{c})$	$h \rightarrow Z\eta_c$
Inclusive	2.0%	2.1%	2.0%
$h$ + jet	3.5%	3.9%	3.7%

**Table 1** The expected 95 % CL limits on the branching fractions of interest for both the inclusive and  $h$  + jet channels, assuming  $3000 \text{ fb}^{-1}$  at  $\sqrt{s} = 13 \text{ TeV}$ .

#### 5 Constraints on the 2HDM parameter space

With a focus on the HL-LHC, we assume the Higgs boson couplings to be tightly constrained to SM-like values. Assuming no evidence for new physics in the HL-LHC data, any 2HDM scenario compatible with the

observations would therefore necessarily be close to the alignment limit. It has been pointed out in Ref. [5] that a light pseudoscalar  $A$  with mass below 10 GeV can be accommodated in this limit, particularly in Type I models, which we consider here. A pseudoscalar that light can decay into pairs of fermions through tree-level interactions or into pairs of gluons and photons through loop-induced couplings. In Type I models, the tree-level couplings to fermions are essentially given by the fermion masses times a universal factor of  $\cot(\beta)$ . A considerable hadronic branching fraction hence arises from decays into quark pairs, gluon pairs, or indirectly from decays into pairs of tau leptons that decay into hadrons subsequently. As shown in Fig. 1, the performance of our analysis is fairly insensitive to the details of the hadronic decay mode of the pseudoscalar. The results of our analysis can therefore directly be used in order to constrain such models. To the best of our knowledge, no detailed analysis of this final state has been provided in the literature so far.

In order to assess the constraining power of our results, we perform a parameter scan for a fixed benchmark pseudoscalar mass of  $m_A = 4 \text{ GeV}$ . For the chosen benchmark value of  $m_A$ , decays into tau leptons and charm quarks dominate. Decays into gluon pairs contribute a branching fraction at the per cent level. Overall, we obtain  $\mathcal{BR}(A \rightarrow \text{hadrons}) \approx 82 \%$ .

In our parameter scan, we calculate the branching ratio relevant for the interpretation of our results,  $\mathcal{BR}(h \rightarrow ZA)$ , for each parameter point. The corresponding partial decay width is given by

$$\Gamma(h \rightarrow ZA) = \frac{|\mathbf{p}|}{8\pi m_h^2} |\mathcal{M}(h \rightarrow ZA)|^2 = \frac{g_{hZA}^2}{2\pi} \frac{|\mathbf{p}|^3}{m_Z^2}, \quad (1)$$

at tree level, where  $\mathbf{p}$  is the three-momentum of either of the two decay products in the rest frame of the Higgs boson. The  $hZA$ -coupling is given by

$$g_{hZA} = \frac{e \cos(\beta - \alpha)}{2 \cos \theta_W \sin \theta_W}. \quad (2)$$

The partial decay width  $\Gamma(h \rightarrow ZA)$  therefore vanishes in the strict alignment limit with  $\cos(\beta - \alpha) = 0$ . The corresponding branching fraction, however, becomes sizable already for small  $\cos(\beta - \alpha)$  if the decay  $h \rightarrow AA$  does not contribute substantially to the Higgs boson total width. We therefore focus on the parameter region, where  $g_{h_{\text{SM}}AA} = 0$  at tree level, which implies [28]

$$m_{12}^2 = (2m^2 + m_h^2) \sin(2\beta)/4.0. \quad (3)$$

To ensure alignment, we perform a uniform scan with  $\sin(\beta - \alpha) \in [0.99, 1.0]$ . In this regime, we can assume the production cross sections of the 125 GeV Higgs to

be SM-like and directly apply our previously obtained limit on  $\mathcal{BR}(h \rightarrow ZA)$ . Note, however, that the limit must be applied to  $\mathcal{BR}(h \rightarrow ZA) \times \mathcal{BR}(A \rightarrow \text{hadrons})$ , since  $\mathcal{BR}(A \rightarrow \text{hadrons}) = 1$  was assumed previously. The remaining free parameters of the model are uniformly varied in the intervals  $m_H \in [130, 600]\text{GeV}$ ,  $m_{H^\pm} \in [50, 600]\text{GeV}$ , and  $\tan\beta \in [0.1, 5.0]$ . We calculate the physical spectrum and the relevant branching fractions with 2HDMC version 1.7.0 [29].

For each point we check for vacuum stability of the potential, tree-level unitarity using the corresponding functionalities of 2HDMC. On the phenomenological side, we check for compatibility of the resulting oblique parameters  $S, T, U$  [30, 31], as calculated by 2HDMC, with electroweak constraints [32]. Only points that can be accommodated within these constraints are retained. Points that are incompatible with exclusion limits set by LEP, Tevatron, and LHC analyses are also rejected. For this purpose, we employ numerical program Higgs-Bounds [33–36] and include all analyses implemented in version 4.3.1. Only parameter points for which none of the scalars in the spectrum can be excluded at 95% CL are retained in our scan. In order to check the compatibility with the LHC and Tevatron Higgs boson signals in our scan, we employ the HiggsSignals program [37, 38] version 1.4.0. We discard any points that are excluded at 95% confidence level based on the  $\chi^2$  calculated by HiggsSignals.

In Fig. 5, we illustrate the results of the parameter scan. We display the distribution of all parameter points that pass the applied theoretical and phenomenological constraints in a two-dimensional parameter plane spanned by  $\cos^2(\beta - \alpha)$  and  $\mathcal{BR}(h \rightarrow ZA) \times \mathcal{BR}(A \rightarrow \text{hadrons})$  along with the tree-level functional dependence of these quantities given by Eq. (1), assuming for simplicity  $\Gamma_{\text{tot}}^h = \Gamma_{\text{tot}}^{h\text{SM}}$ . For large  $\cos(\beta - \alpha)$ , this is assumption is violated due to the opening of further decay channels. At small  $\cos(\beta - \alpha)$ , however, the corresponding approximation proves to be reasonable for parameter points that pass the applied phenomenological constraints. As illustrated in Fig. 5, the scanned parameter space can effectively be constrained to very small values of  $\cos^2(\beta - \alpha)$  by applying our expected limit on  $\mathcal{BR}(h \rightarrow ZA)$ . In fact, we find that no parameter point with  $\cos^2(\beta - \alpha) > 0.0035$  survives the limit set by the analysis presented above, translating to  $\sin(\beta - \alpha) \gtrsim 0.998$  in the scanned subspace of parameters. Correspondingly, a mere 12% of the parameter points displayed in Fig. 5 fall in the region of allowed values for  $\mathcal{BR}(h \rightarrow ZA) \times \mathcal{BR}(A \rightarrow \text{hadrons})$  after applying the limit on  $\mathcal{BR}(h \rightarrow ZA)$  obtained above.

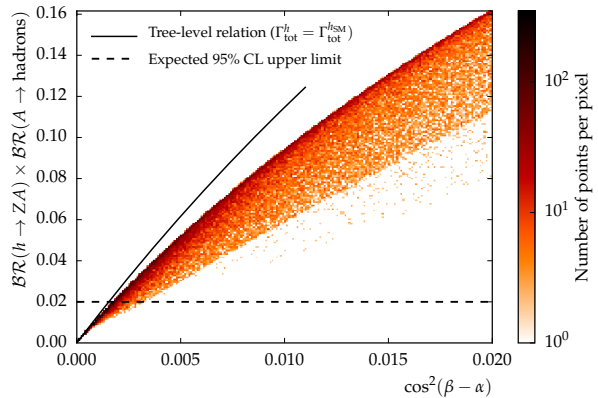


**Fig. 5** Distribution of scanned parameter points in the  $\cos^2(\beta - \alpha)$  vs.  $\mathcal{BR}(h \rightarrow ZA) \times \mathcal{BR}(A \rightarrow \text{hadrons})$  plane. The color-coding denotes the density of points in the respective areas as indicated by the color bar. We also display the tree-level functional relationship between  $\cos^2(\beta - \alpha)$  and  $\mathcal{BR}(h \rightarrow ZA) \times \mathcal{BR}(A \rightarrow \text{hadrons})$ , assuming  $\Gamma_{\text{tot}}^h = \Gamma_{\text{tot}}^{h\text{SM}}$ . The dashed line shows the expected 95% CL upper limit on the displayed branching fraction. All points above this line are expected to be excluded by the analysis presented here.

## 6 Summary

Searches for rare and exclusive Higgs boson decays are at the core of the program of the High Luminosity LHC. The observation of Higgs boson decays into light elementary or composite resonances would be evidence for the existence of physics beyond the Standard Model.

While previous experimental strategies to reconstruct light resonances relied entirely on their leptonic decay products, in this work, we evaluated the prospects for their discovery in the often dominant hadronic decay channels. We have focused on the Higgs boson production processes with the largest cross sections,  $pp \rightarrow h$  and  $pp \rightarrow h + \text{jet}$ , with subsequent decays  $h \rightarrow ZA$  or  $h \rightarrow Z\eta_c$ . The former is present in many multi-Higgs extensions of the Standard Model, while observing the latter at a branching ratio of  $\mathcal{BR}(h \rightarrow Z\eta_c) \geq 10^{-3}$  could indicate an enhanced Higgs-charm coupling.

The decay products of light resonances with masses below a few GeV that arise from Higgs decays are highly collimated, i.e. they get emitted into a small area of the detector. In such scenarios jet substructure is an indispensable tool to retain sensitivity in discriminating signal from large QCD-induced backgrounds. In particular, by exploiting the improved angular resolution of track-based observables, a good signal-to-background discrimination can be achieved, which results in a limit on the branching ratios of  $\mathcal{O}(1)\%$  for a data sample corresponding to  $3000\text{fb}^{-1}$  at  $\sqrt{s} = 13\text{TeV}$ .

## Acknowledgments

SK's work was supported by the European Union as part of the FP7 Marie Curie Initial Training Network MCnetITN (PITN-GA-2012-315877). AC and KN are supported in part by the European Union's FP7 Marie Curie Career Integration Grant EWSB (PCIG12-GA-2012-334034). This work was made possible thanks to the Institute of Particle Physics Phenomenology Associate scheme.

## References

1. ATLAS collaboration, *Observation of a new particle in the search for the Standard Model Higgs boson with the ATLAS detector at the LHC*, *Phys. Lett.* **B716** (2012) 1–29, [[1207.7214](#)].
2. CMS collaboration, *Observation of a new boson at a mass of 125 GeV with the CMS experiment at the LHC*, *Phys. Lett.* **B716** (2012) 30–61, [[1207.7235](#)].
3. ATLAS, CMS collaboration, *Measurements of the Higgs boson production and decay rates and constraints on its couplings from a combined ATLAS and CMS analysis of the LHC pp collision data at  $\sqrt{s} = 7$  and 8 TeV*, [1606.02266](#).
4. D. Curtin et al., *Exotic decays of the 125 GeV Higgs boson*, *Phys. Rev.* **D90** (2014) 075004, [[1312.4992](#)].
5. J. Bernon, J. F. Gunion, H. E. Haber, Y. Jiang and S. Kraml, *Scrutinizing the alignment limit in two-Higgs-doublet models:  $m_h = 125$  GeV*, *Phys. Rev.* **D92** (2015) 075004, [[1507.00933](#)].
6. D. Curtin, R. Essig, S. Gori and J. Shelton, *Illuminating Dark Photons with High-Energy Colliders*, *JHEP* **02** (2015) 157, [[1412.0018](#)].
7. G. T. Bodwin, F. Petriello, S. Stoynev and M. Velasco, *Higgs boson decays to quarkonia and the  $H\bar{c}c$  coupling*, *Phys. Rev.* **D88** (2013) 053003, [[1306.5770](#)].
8. A. L. Kagan, G. Perez, F. Petriello, Y. Soreq, S. Stoynev and J. Zupan, *Exclusive Window onto Higgs Yukawa Couplings*, *Phys. Rev. Lett.* **114** (2015) 101802, [[1406.1722](#)].
9. G. Isidori, A. V. Manohar and M. Trott, *Probing the nature of the Higgs-like Boson via  $h \rightarrow V\mathcal{F}$  decays*, *Phys. Lett.* **B728** (2014) 131–135, [[1305.0663](#)].
10. M. König and M. Neubert, *Exclusive Radiative Higgs Decays as Probes of Light-Quark Yukawa Couplings*, *JHEP* **08** (2015) 012, [[1505.03870](#)].
11. ATLAS collaboration, *Search for Higgs and Z Boson Decays to  $J/\psi$  and  $\Upsilon(nS)$  with the ATLAS Detector*, *Phys. Rev. Lett.* **114** (2015) 121801, [[1501.03276](#)].
12. CMS collaboration, *Search for a Higgs boson decaying into  $\gamma^*\gamma \rightarrow \ell\ell\gamma$  with low dilepton mass in pp collisions at  $\sqrt{s} = 8$  TeV*, *Phys. Lett.* **B753** (2016) 341–362, [[1507.03031](#)].
13. ATLAS collaboration, *Search for Higgs and Z Boson Decays to  $\phi\gamma$  with the ATLAS Detector*, *Phys. Rev. Lett.* **117** (2016) 111802, [[1607.03400](#)].
14. PARTICLE DATA GROUP collaboration, K. A. Olive et al., *Review of Particle Physics*, *Chin. Phys.* **C38** (2014) 090001.
15. A. Katz, M. Son and B. Tweedie, *Jet Substructure and the Search for Neutral Spin-One Resonances in Electroweak Boson Channels*, *JHEP* **03** (2011) 011, [[1010.5253](#)].
16. S. Schätzel and M. Spannowsky, *Tagging highly boosted top quarks*, *Phys. Rev.* **D89** (2014) 014007, [[1308.0540](#)].
17. A. J. Larkoski, F. Maltoni and M. Selvaggi, *Tracking down hyper-boosted top quarks*, *JHEP* **06** (2015) 032, [[1503.03347](#)].
18. M. Spannowsky and M. Stoll, *Tracking New Physics at the LHC and beyond*, *Phys. Rev.* **D92** (2015) 054033, [[1505.01921](#)].
19. ATLAS collaboration, *The ATLAS Experiment at the CERN Large Hadron Collider*, *JINST* **3** (2008) S08003.
20. CMS collaboration, *The CMS experiment at the CERN LHC*, *JINST* **3** (2008) S08004.
21. T. Gleisberg, S. Höche, F. Krauss, M. Schönherr, S. Schumann, F. Siegert et al., *Event generation with SHERPA 1.1*, *JHEP* **02** (2009) 007, [[0811.4622](#)].
22. M. Buschmann, D. Goncalves, S. Kuttimalai, M. Schonherr, F. Krauss and T. Plehn, *Mass Effects in the Higgs-Gluon Coupling: Boosted vs Off-Shell Production*, *JHEP* **02** (2015) 038, [[1410.5806](#)].
23. S. Höche, S. Kuttimalai, S. Schumann and F. Siegert, *Beyond Standard Model calculations with Sherpa*, *Eur. Phys. J.* **C75** (2015) 135, [[1412.6478](#)].
24. C. Degrande, C. Duhr, B. Fuks, D. Grellscheid, O. Mattelaer and T. Reiter, *UFO - The Universal FeynRules Output*, *Comput. Phys. Commun.* **183** (2012) 1201–1214, [[1108.2040](#)].
25. S. Höche, F. Krauss, M. Schönherr and F. Siegert, *QCD matrix elements + parton showers: The NLO case*, *JHEP* **04** (2013) 027, [[1207.5030](#)].
26. DELPHES 3 collaboration, J. de Favereau, C. Delaere, P. Demin, A. Giammanco, V. Lematre, A. Mertens et al., *DELPHES 3, A modular*

- 
- framework for fast simulation of a generic collider experiment, *JHEP* **02** (2014) 057, [[1307.6346](#)].
27. A. Hoecker et al., *TMVA - Toolkit for Multivariate Data Analysis*, *PoS ACAT* (2007) 040, [[physics/0703039](#)].
  28. M. Casolino, T. Farooque, A. Juste, T. Liu and M. Spannowsky, *Probing a light CP-odd scalar in di-top-associated production at the LHC*, *Eur. Phys. J.* **C75** (2015) 498, [[1507.07004](#)].
  29. D. Eriksson, J. Rathsman and O. Stål, *2HDMC: Two-Higgs-Doublet Model Calculator Physics and Manual*, *Comput. Phys. Commun.* **181** (2010) 189–205, [[0902.0851](#)].
  30. M. E. Peskin and T. Takeuchi, *A New constraint on a strongly interacting Higgs sector*, *Phys. Rev. Lett.* **65** (1990) 964–967.
  31. M. E. Peskin and T. Takeuchi, *Estimation of oblique electroweak corrections*, *Phys. Rev.* **D46** (1992) 381–409.
  32. GFITTER GROUP collaboration, M. Baak et al., *The global electroweak fit at NNLO and prospects for the LHC and ILC*, *Eur. Phys. J.* **C74** (2014) 3046, [[1407.3792](#)].
  33. P. Bechtle, O. Brein, S. Heinemeyer, G. Weiglein and K. E. Williams, *HiggsBounds: Confronting Arbitrary Higgs Sectors with Exclusion Bounds from LEP and the Tevatron*, *Comput. Phys. Commun.* **181** (2010) 138–167, [[0811.4169](#)].
  34. P. Bechtle, O. Brein, S. Heinemeyer, G. Weiglein and K. E. Williams, *HiggsBounds 2.0.0: Confronting Neutral and Charged Higgs Sector Predictions with Exclusion Bounds from LEP and the Tevatron*, *Comput. Phys. Commun.* **182** (2011) 2605–2631, [[1102.1898](#)].
  35. P. Bechtle et al., *Recent Developments in HiggsBounds and a Preview of HiggsSignals*, *PoS CHARGED2012* (2012) 024, [[1301.2345](#)].
  36. P. Bechtle, S. Heinemeyer, O. Stål, T. Stefaniak and G. Weiglein, *Applying Exclusion Likelihoods from LHC Searches to Extended Higgs Sectors*, *Eur. Phys. J.* **C75** (2015) 421, [[1507.06706](#)].
  37. P. Bechtle, S. Heinemeyer, O. Stål, T. Stefaniak and G. Weiglein, *HiggsSignals: Confronting arbitrary Higgs sectors with measurements at the Tevatron and the LHC*, *Eur. Phys. J.* **C74** (2014) 2711, [[1305.1933](#)].
  38. P. Bechtle, S. Heinemeyer, O. Stål, T. Stefaniak and G. Weiglein, *Probing the Standard Model with Higgs signal rates from the Tevatron, the LHC and a future ILC*, *JHEP* **11** (2014) 039, [[1403.1582](#)].

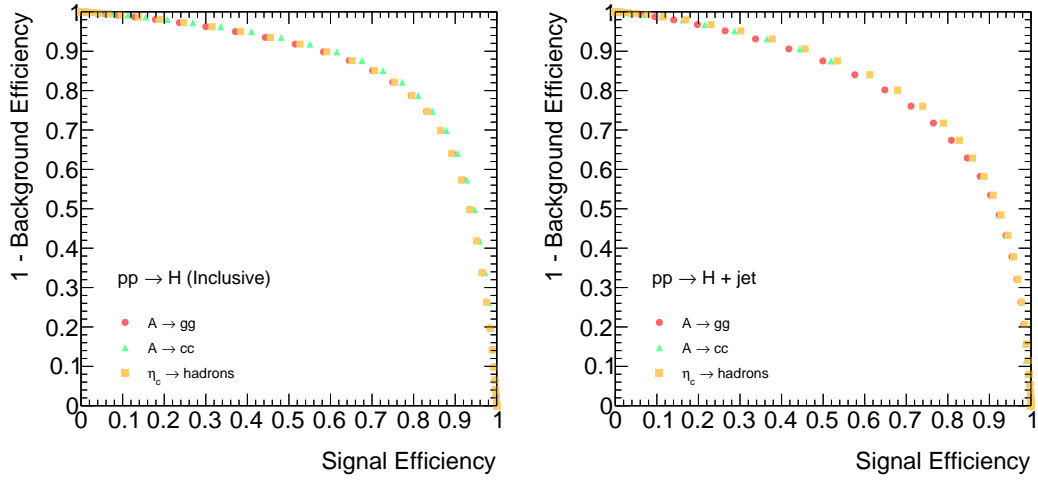


**Fig. 1** The background rejection as a function of signal efficiency for the low mass resonances considered for the inclusive (left) and  $h + \text{jet}$  (right) production channels.

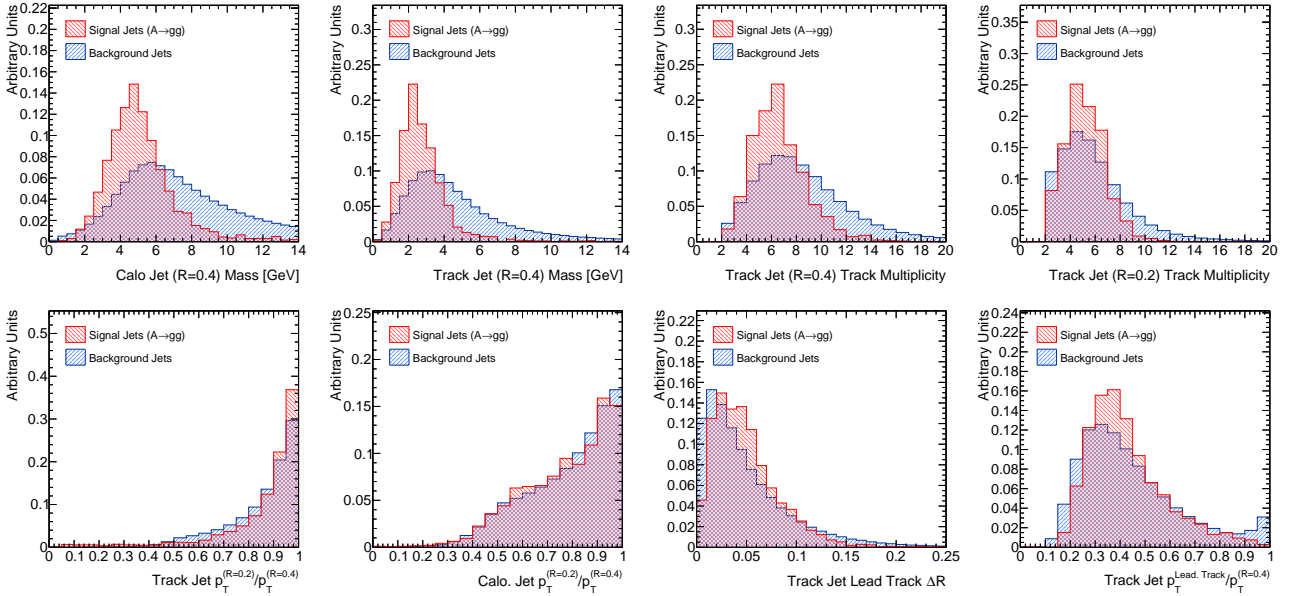


**Fig. 2** Distributions of eight of the variables used as input to the BDT training for jets from  $A \rightarrow gg$  decays and jets produced in association with  $Z$  bosons.



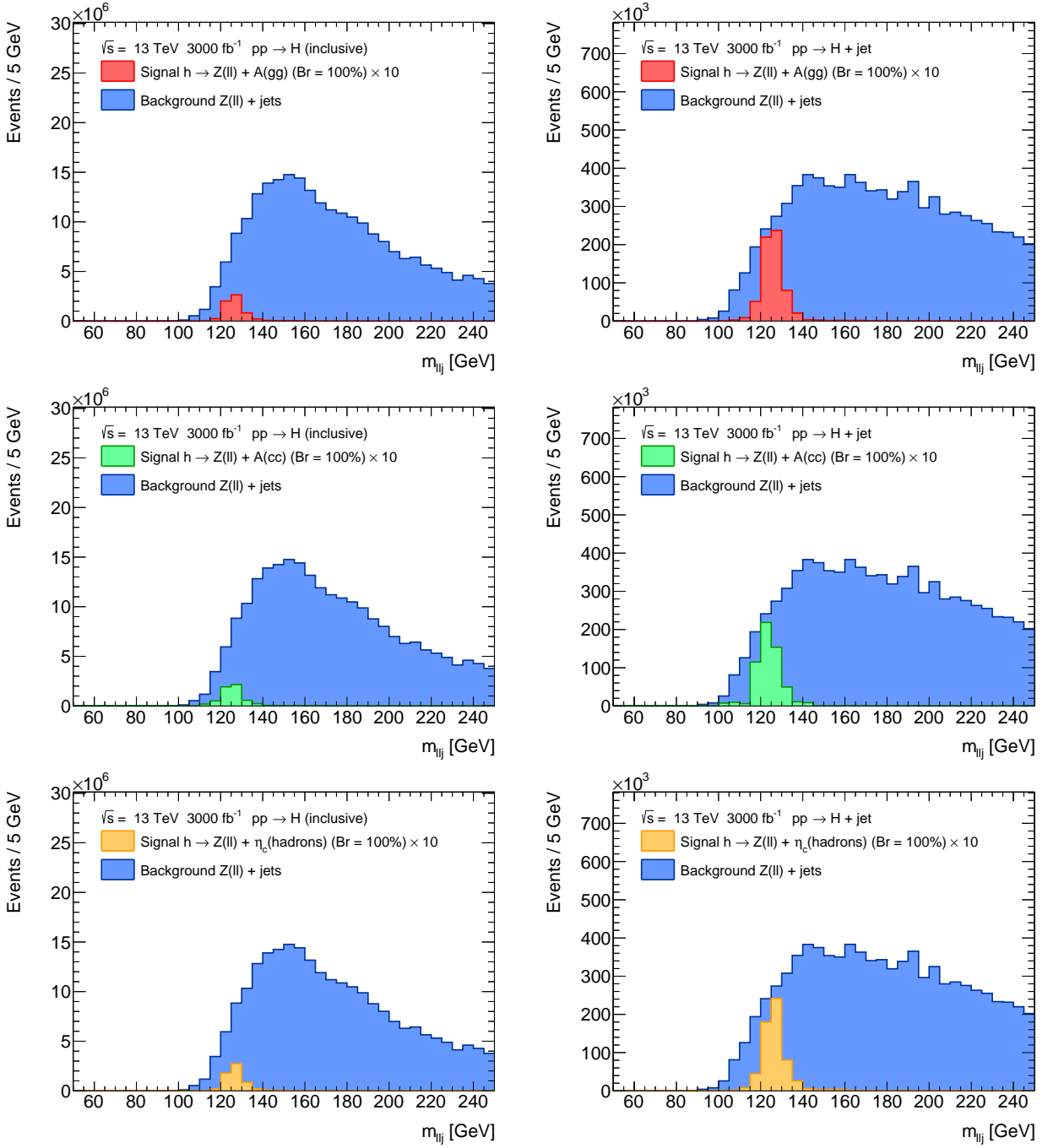


**Fig. 3** The invariant mass distribution of the jet-dilepton system (with no BDT based selection applied) in inclusive  $h$  production (left) and  $h + \text{jet}$  production (right) is shown for  $A \rightarrow gg$  (top),  $A \rightarrow c\bar{c}$  (middle) and  $\eta_c \rightarrow \text{hadrons}$  (bottom) signals in comparison to the background contribution. The signal contribution is multiplied by ten to improve visibility.

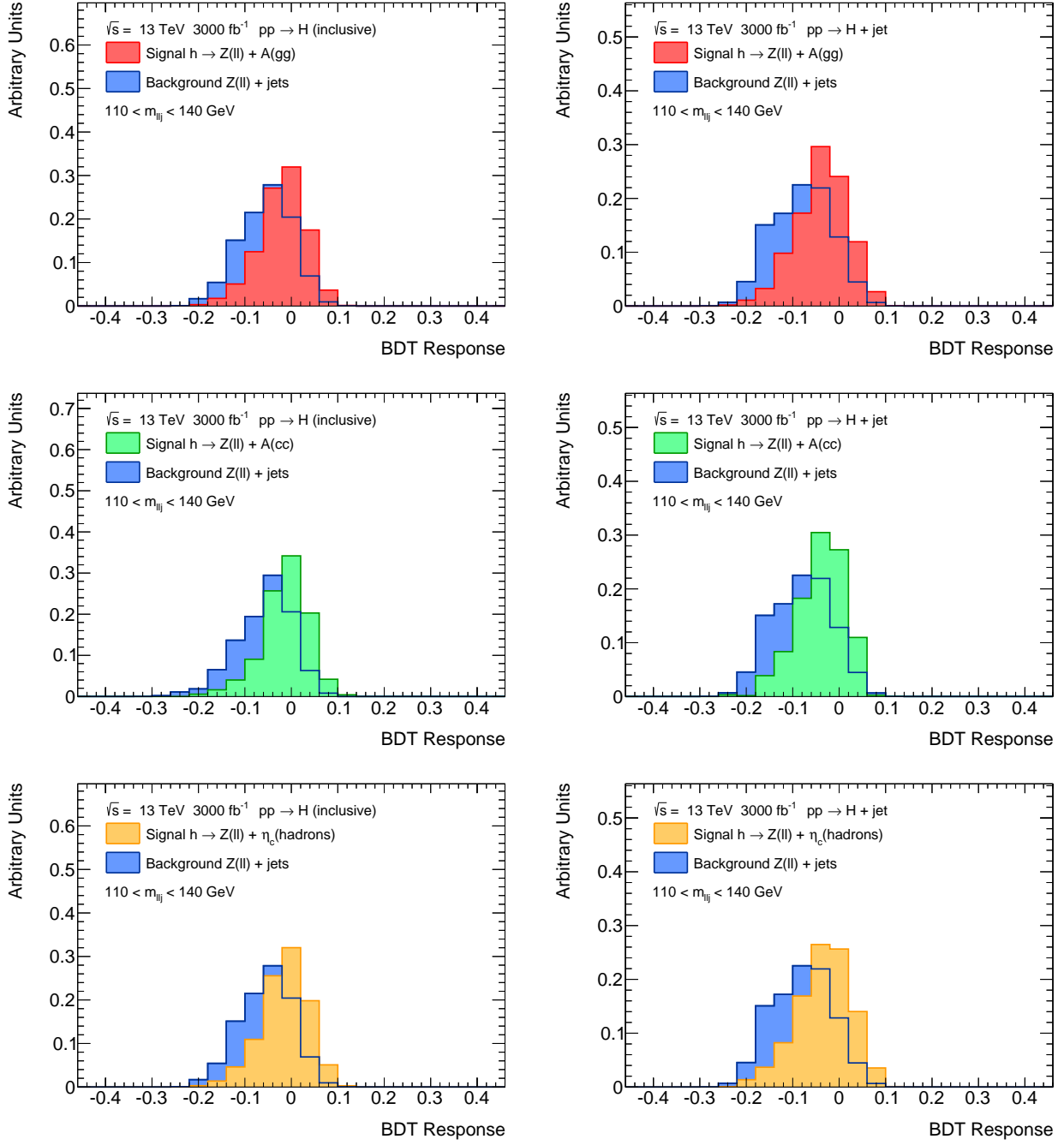


**Fig. 4** The normalised BDT response for the inclusive (left) and  $h + \text{jet}$  (right) production shown for  $A \rightarrow gg$  (top),  $A \rightarrow c\bar{c}$  (middle) and  $\eta_c \rightarrow \text{hadrons}$  (right) in comparison to the background.